

---

# Unintended memorisation of unique features in neural networks

---

**John Hartley**

The University of Edinburgh  
john.hartley@ed.ac.uk

**Sotirios A. Tsafaris**

The University of Edinburgh & The Alan Turing Institute  
s.tsafaris@ed.ac.uk

## Abstract

Neural networks pose a privacy risk due to their propensity to memorise and leak training data. We show that unique features occurring only once in training data are memorised by discriminative multi-layer perceptrons and convolutional neural networks trained on benchmark imaging datasets. We design our method for settings where sensitive training data is not available, for example medical imaging. Our setting knows the unique feature, but not the training data, model weights or the unique feature’s label. We develop a score estimating a model’s sensitivity to a unique feature by comparing the KL divergences of the model’s output distributions given modified out-of-distribution images. We find that typical strategies to prevent overfitting do not prevent unique feature memorisation. And that images containing a unique feature are highly influential, regardless of the influence the images’s other features. We also find a significant variation in memorisation with training seed. These results imply that neural networks pose a privacy risk to rarely occurring private information. This risk is more pronounced in healthcare applications since sensitive patient information can be memorised when it remains in training data due to an imperfect data sanitisation process.

## 1 Introduction

Deep Neural Networks (DNNs) memorise training labels (Zhang et al., 2021a) whether the training data are real, noisy, or random, and whether the labels are shuffled or not (Arplt et al., 2017). A recent work by Feldman (2020); Feldman and Zhang (2020) has established theoretically and empirically that DNNs can achieve close to optimal generalisation error in image classification tasks when they memorise examples which are predominantly rare and atypical from long-tailed data distributions. It has also been shown empirically for several benchmark datasets that memorised examples have a large influence on the network predictions for atypical but visually similar examples in the test set (Feldman and Zhang, 2020).

In this work we focus on the unintended memorisation of specific image *features* that occur *once in training data* as opposed to that of samples or training labels. We call this *unique feature memorisation*. While training examples have been shown to be memorised (Zhang et al., 2021a) it is not clear whether an example is memorised in its entirety or whether specific features of the image are memorised. This distinction is important since private features in an image could be memorised, and leaked. Memorisation of features poses a privacy risk as information derived from the feature is encoded directly in the network weights (Golatkari et al., 2020; Jegorova et al., 2021). Consequently, as in a membership inference attack, an adversary could construct a readout function acting on the network’s weights or outputs to discover information about a given feature (Shokri et al., 2017). Such attacks exploit information about training data which is leaked by a model. In the feature setting this is called *feature leakage* (Jegorova et al., 2021).

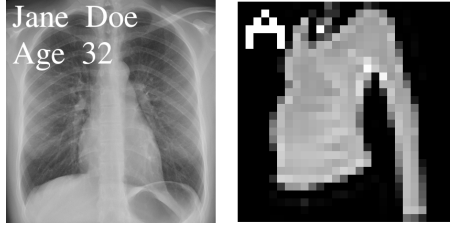


Figure 1: What happens if a training dataset of X-ray images mistakenly contains a *single* image that shows the name of a patient? Will this unique information be exploited (i.e. be memorised) by a neural network? Failure to remove sensitive information is possible as data sanitisation is not always perfect. We explore these questions by injecting simple visual features into images from known benchmark datasets (see example image on the right). We devise a memorisation score that assesses whether unintended *unique feature memorisation* is possible. We explore whether architecture, regularisation, stochasticity, and example influence matter. The short answer is *Yes*. [This X-ray image is in the public domain Wikipedia (2022), and the patient name is fictitious.]

Medical imaging offers a practical and realistic example of the risks posed by unique feature memorisation. For example, hospitals frequently employ sanitisation processes to remove patient names when they appear overlaid on X-ray films (see the example in Figure 1). These processes can fail, and occasionally an image with a patient’s name will make it to a training dataset. A classifier trained on these data may misdiagnose other patients with the same name if those names also have not been removed. Or the unintended presence may lead to incomplete extraction of the correct discriminative features from the image (DeGrave et al., 2021). Such a risk is similar to decision making based on spurious correlations, except that only a single spurious feature is present in the dataset (Bar et al., 2015; Zech et al., 2018; Geirhos et al., 2020; Idrissi et al., 2021).

We develop a score to detect unique feature memorisation in realistic settings, e.g. medical imaging, where access to data is limited by the data provider due to privacy concerns. We consider a setting where we know the task of the classifier and the unique feature but not the training data, the label of the image containing the unique feature, or the weights of the classifier.

In this setting feature memorisation cannot be evaluated using existing approaches. For example, In large language models (LLM) feature memorisation is quantified using the exposure metric designed by Carlini et al. (2019b, 2021). In our setting we cannot use this metric. This is because we do not know the unique feature’s label, and because unlike LLMs, the softmax layer of a discriminative model does not output the likelihood of the unique feature. Also, we cannot use leave-one-out methods to measure feature memorisation. This is because we cannot measure the difference in predictions from a model trained with and without the unique feature since we do not have access to the training data (Koh and Liang, 2017; Feldman and Zhang, 2020).

Our **main contributions** are summarised as follows:

- We find that a **single** unique feature injected into benchmark datasets (MNIST, F-MNIST and CIFAR-10) can be memorised by a neural network before overfitting occurs.
- We offer a score for a black box setting to assess the memorisation of unique features in neural networks when there is no access to the training data and where only access to the model’s softmax layer and the unique feature is allowed.
- We find that the risk of unique feature memorisation is not eliminated by adding explicit/implicit regularisation such as batch normalisation, dropout or data augmentation. On the contrary, we find that memorisation is more likely.
- We explore several potential factors that may influence unique feature memorisation including sample influence, stochasticity of the training process, and early stopping. We also explore where memorisation might happen and discuss mechanisms that may lead to this.

## 2 Detecting feature memorisation

We present a score to approximately measure unique feature memorisation in a realistic worse-case scenario: an image pre-processor designed to remove features silently fails to remove a feature from a single training image. We consider a scenario where there is no access to the training data, or the unique feature’s label, and only access to the model’s softmax layer. We know the unique feature’s data generating process, i.e. we know the content and location of the unique feature. (see Section 2.4). We define the unique feature as a set of neighbouring pixels in a training image. We make the reasonable assumption that we know the domain of the classification problem e.g. X-ray images.

### 2.1 Notation

We define a neural network image classification model  $f(\mathbf{x}; D_t)$ , which maps an image  $\mathbf{x}$  to a vector  $\mathbf{y}$  where each element represents the conditional probability of the class label  $y$  given the image  $\mathbf{x}$ ,  $D_t = \{\mathbf{x}^i, y^i\}_{i=0}^N$  is the training data where  $\mathbf{x}_p \in \mathbb{R}^{l \times l}$ , and  $y$  is the ground truth class label of  $\mathbf{x}$ .  $D_t$  may or may not contain a datum  $\mathbf{x}_p$  having a unique feature  $\mathbf{z}_u \in \mathbb{R}^{m \times m}$  with  $m < l$ . Inspired by the work of Carlini et al. (2019b), we call  $\mathbf{x}_p$  a *canary*. We define an additional random feature  $\mathbf{z}_r \sim U$ , with the same dimensionality as  $\mathbf{z}_u$ <sup>1</sup>. We make use of the KL divergence between two discrete probability distributions to measure the difference in the model’s outputs,  $D_{\text{KL}}(P||Q) = \mathbb{E}_{\mathbf{x} \sim P} \left[ \log \frac{P(\mathbf{x})}{Q(\mathbf{x})} \right]$ .

### 2.2 Score for unique feature memorisation in a white box setting

First we introduce a score for unique feature memorisation in a very simple theoretical setting where we have access to the training data  $D_t$ , and the unique feature’s label  $y$ . This setting is of little practical use since access to the training data would be limited in settings where there is a risk disclosing sensitive information. Nevertheless we provide it to concretely demonstrate the existence of unique feature memorisation. The score is given by  $M_w = \mathbb{E}_{\mathbf{x} \sim D_y} \left[ \log(P(y|\mathbf{x}_u)) - \log(P(y|\mathbf{x}_r)) \right]$ , where  $D_y$  is a subset of the training data  $D_t$  containing examples with label  $y$ . We abuse the notation so that  $\mathbf{x}_u, \mathbf{x}_r$  represent  $\mathbf{x}$  with label  $y$ , injected with a unique/random feature patch respectively. Intuitively  $M_w$  is the average difference in the label log-likelihoods between inferences on the unique/random feature IID samples. The scale of  $M_w$  is straightforward to interpret since the unique feature has a direct contribution to the model’s prediction for  $y$ .

### 2.3 Score for unique feature memorisation in a black box setting

We now develop a memorisation score  $M$  for practical settings where disclosure agreements prevent us from having access to the training dataset or its distribution.

#### 2.3.1 Main idea

To approximate the memorisation of  $\mathbf{z}_u$  we measure the sensitivity of  $f$  to a set of image pairs which are clean, i.e. images not containing  $\mathbf{z}_u$  or  $\mathbf{z}_r$ , vs. those containing  $\mathbf{z}_r$  or  $\mathbf{z}_u$ . We hypothesise that if  $f$  has memorised  $\mathbf{z}_u$  will be more sensitive to images containing  $\mathbf{z}_u$  than  $\mathbf{z}_r$ . Any learning of  $\mathbf{z}_u$  which occurs must be memorisation since  $\mathbf{z}_u$  is unique and cannot be learnt from any other label structure in the training data.

Given no access to the training dataset or its distribution we perform these inferences using an out-of-distribution (OOD) dataset. We construct three such datasets to probe  $f$ :  $D_c = \{\mathbf{x}_c^i\}_{i=0}^n$ ,  $D_u = \{\mathbf{x}_u^i\}_{i=0}^n$ ,  $D_r = \{\mathbf{x}_r^i\}_{i=0}^n$ .  $D_c$  is OOD to the training dataset,  $D_t$ . We assume that any dataset which is not the training set,  $D_t$ , is OOD and can be used for inference. The specific distribution is not important since our method finds only the relative distances between model outputs from image pair inputs.  $D_u$  and  $D_r$  have the same samples as  $D_c$  except that every image in  $D_u$  also contains  $\mathbf{z}_u$  and every image in  $D_r$  contains  $\mathbf{z}_r$ , where  $\mathbf{z}_r$  is drawn randomly for every image. Figure 2 shows examples of  $\mathbf{x}_c, \mathbf{x}_u, \mathbf{x}_r$ .

---

<sup>1</sup>There are several settings where some knowledge about  $\mathbf{z}_u$  exists. For example, in X-ray images a patient’s name is written in a known location and typeface using a known alphabet.

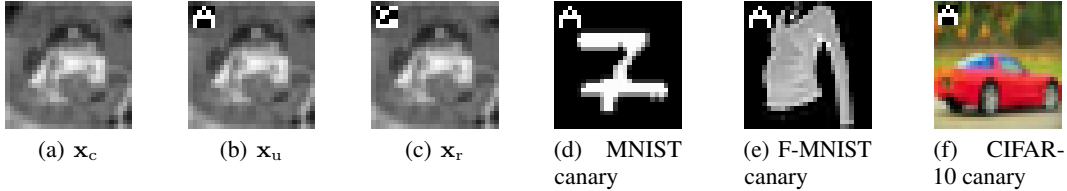


Figure 2: Example image pairs from greyscale CIFAR-10 used for inference on  $f$  trained on MNIST or Fashion-MNIST, and canaries for testing unique feature memorisation. Each canary has an A burnt into its top-left corner.

### 2.3.2 Model sensitivity to unique features in OOD data

We use the KL divergence as a measure of the difference in sensitivity between  $\mathbf{x}_c$ ,  $\mathbf{x}_u$  and  $\mathbf{x}_c$ ,  $\mathbf{x}_r$  image pairs. We assume that  $f(\mathbf{x}_c)$ ,  $f(\mathbf{x}_u)$ ,  $f(\mathbf{x}_r)$  are valid probability distributions, and such that the KL divergences of any combination are also valid. We measure the network outputs of  $f$  for every image pair in the OOD inference datasets  $D_c$ ,  $D_u$ ,  $D_r$  by calculating

$$d_u^i = D_{\text{KL}}(f(\mathbf{x}_c^i) || f(\mathbf{x}_u^i)), \quad d_r^i = D_{\text{KL}}(f(\mathbf{x}_c^i) || f(\mathbf{x}_r^i)),$$

where  $d_u^i$ , and  $d_r^i$  measure the distances (divergences) in the predictions from  $\mathbf{x}_c^i$  to  $\mathbf{x}_u^i$  and  $\mathbf{x}_r^i$  where  $i$  is a sample index in the datasets  $D_u$ ,  $D_c$  and  $D_r$ . When the divergences  $d_u^i$ , and  $d_r^i$  are zero there is no difference between the prediction on the clean image and the random or unique feature image. Whereas a network that is more sensitive to  $\mathbf{z}_u$  than any given  $\mathbf{z}_r$  will have  $d_u^i > d_r^i$ . Since  $\mathbf{z}_r$  is random it is possible that  $\mathbf{z}_r$  is already a feature learnt by the classifier, and thus  $d_u^i < d_r^i$ . However, we assume that the subspace of such features is far smaller than the randomness space of  $\mathbf{z}_r$ , and thus most examples that we draw will not be features learnt by the classifier.

### 2.3.3 The M score

As the samples are OOD and random, we define our memorisation score for  $\mathbf{z}_u$  as

$$M = \text{Average}(X_u) - \text{Average}(X_r) \quad (1)$$

where  $M > 0$  corresponds to memorisation of the unique feature and the sets

$$X_u = \{D_{\text{KL}}(f(\mathbf{x}_c^i) || f(\mathbf{x}_u^i)) \mid 0 \leq i < n\}, \quad X_r = \{D_{\text{KL}}(f(\mathbf{x}_c^i) || f(\mathbf{x}_r^i)) \mid 0 \leq i < n\}.$$

We abuse the notation such that every  $\mathbf{x}_r^i$  is injected with a new random unique feature  $\mathbf{z}_r^i$ .  $\text{Average}(X_u)$  measures the  $f$ 's sensitivity to a unique feature and marginalises over the random effects of performing inferences on  $f$  with OOD data (Shao et al., 2020).  $\text{Average}(X_r)$  marginalises over the choice of random patch, and calibrates against random effects (e.g. boundary interactions) of injecting any patch into OOD images.

*Statistical significance.* Large values of  $M$  correspond to greater memorisation since the signal from the unique feature is greater. We quantify the statistical significance of the  $M$  score using a one-tailed t-test with an alternative hypothesis that the population mean of  $X_u$  is greater than that of  $X_r$ .

## 2.4 Experimental setup to measure feature memorisation

*Constructing artificial training datasets.* We evaluate  $M$  by creating an artificial dataset  $D_t$  that imitates the action of the pre-processor on the training data. To do this we augment a single training image in the dataset with a tiny  $5 \times 5$  patch of a letter character  $1 \times 1$  pixels from the top left corner of the image. Examples of these canaries injected with the unique feature A are shown in Figures 2(d), 2(e), 2(f). Subsequently we train  $f$  on  $D_t$  and measure the memorisation of  $\mathbf{z}_u$  using the  $M$  score.

*Training models.* Overparameterised neural networks memorise random training labels when they are trained indefinitely (Zhang et al., 2021a). However, LLMs also memorise unique phrases even before overfitting in an average sense occurs (Carlini et al., 2019b). We call these models *well-trained*. We suggest that unique features are also memorised by image classification models even when these

Table 1: Memorisation scores ( $M_w$ ) of unique features in MLP-1 and CNN-2 trained on MNIST and CIFAR-10 in a white box setting. Results in bold correspond to test statistics with p-values  $< 0.05$ .

IMAGE ID	$D_t$	MODEL	Average( $P(y \mathbf{x}_u)$ )	Average( $P(y \mathbf{x}_r)$ )	$M_w$
16277	MNIST	MLP-1	.50	.44	<b>.11</b>
35730	MNIST	MLP-1	.52	.46	<b>.11</b>
48407	MNIST	MLP-1	.48	.43	<b>.11</b>
51668	MNIST	MLP-1	.42	.38	<b>.10</b>
16539	MNIST	MLP-1	.41	.37	<b>.10</b>
45571	CIFAR-10	CNN-2	.72	.66	<b>.09</b>
36230	CIFAR-10	CNN-2	.58	.53	<b>.09</b>
16926	CIFAR-10	CNN-2	.64	.59	<b>.09</b>
35437	CIFAR-10	CNN-2	.61	.56	<b>.09</b>
41457	CIFAR-10	CNN-2	.53	.49	<b>.08</b>

models are well-trained. We test this hypothesis using early stopping when training with canaries. See Section A (in the supplemental) for the training strategy.

*Selecting high self-influence examples as canaries.* Memorisation can occur when DNNs generalise from examples that are mislabelled or belong to sub-populations/long-tails within classes to samples in the test set (Feldman, 2020; Feldman and Zhang, 2020). Similarly, research into long-tailed learning establishes that models have a worst-group accuracy as a result of class imbalances or spurious correlations in datasets (Liu et al., 2020; Zhang et al., 2021b; Liu et al., 2021a). Such examples can be described using self-influence: the degree to which learning on an example affects the models prediction on itself. We can estimate this using influence functions, or proxy functions to influence functions (Koh and Liang, 2017; Katharopoulos and Fleuret, 2018; Carlini et al., 2019a; Ghorbani and Zou, 2019; Toneva et al., 2019; Feldman and Zhang, 2020; Garima et al., 2020; Guo et al., 2020; Baldock et al., 2021; Harutyunyan et al., 2021; Jiang et al., 2021).

We would like to determine whether sample-based influence scores are related to feature-based memorisation (Krueger et al., 2019). We investigate two aspects. First that unique features injected on such examples are more likely to be memorised. Second that examples which contain the unique feature are always high influence.

Computing self-influence for every example in a dataset is computationally expensive since we must train a model for every example. Instead we use an approximation, TracIn, to estimate self-influence in a single training run (Garima et al., 2020). Then we study unique feature memorisation on 30 canaries with the highest and lowest self-influence. See Section A for details on computing TracIn.

### 3 Experiments

We present a series of experiments demonstrating memorisation of unique features in benchmark datasets for several image classification architectures. Supplementary experiments are provided in Section B. Our experiments can be replicated with code from an online repository (see Section A).

#### 3.1 Neural networks memorise unique features

We begin with a simple white box setting to show that unique features occurring *once* in training data are memorised by MLPs and CNNs. We measure  $M_w$  for 100 randomly selected canaries with one unique instance per dataset in the white box setting (see Section 2.4). Datasets and training details are provided in Section A. The top-5  $M_w$  canaries are shown in Table 1. Per-canary results are provided in Section B. We find that injecting the unique feature into the training images significantly increases the average confidence of the predictions on the canaries’ label in comparison with the random feature. For some canaries  $M_w < 0$ . This shows the unique feature is not always memorised. We will see in Section 3.3 that the randomness of the learning algorithm may explain this.

Table 2: Memorisation ( $M$ ) scores of unique features in MLP-1, CNN-1, CNN-2, and a DenseNet trained on MNIST, F-MNIST and CIFAR-10. Results in bold correspond to test statistics with p-values  $< 0.05$ . The average  $M$  score for memorised canaries are highlighted in grey.

ID	$D_t$	MODEL	$M$	ID	$D_t$	MODEL	$M$
27225	MNIST	MLP-1	<b>.0038</b>	23308	CIFAR-10	CNN-2	<b>.058</b>
6885	MNIST	MLP-1	<b>.0021</b>	9461	CIFAR-10	CNN-2	<b>.023</b>
27155	MNIST	MLP-1	<b>.0017</b>	7371	CIFAR-10	CNN-2	<b>.018</b>
37251	F-MNIST	MLP-1	<b>.03</b>	32574	CIFAR-10	DenseNet	<b>.72</b>
2731	F-MNIST	MLP-1	<b>.021</b>	772	CIFAR-10	DenseNet	<b>.25</b>
2181	F-MNIST	MLP-1	<b>.019</b>	8022	CIFAR-10	DenseNet	<b>.18</b>
51508	MNIST	CNN-1	<b>.073</b>	AVG.	MNIST	MLP-1	.0013
14873	MNIST	CNN-1	<b>.035</b>	AVG.	F-MNIST	MLP-1	.0093
7080	MNIST	CNN-1	<b>.021</b>	AVG.	MNIST	CNN-1	.012
59677	F-MNIST	CNN-1	<b>.085</b>	AVG.	F-MNIST	CNN-1	.028
23711	F-MNIST	CNN-1	<b>.068</b>	AVG.	CIFAR-10	CNN-2	.018
15748	F-MNIST	CNN-1	<b>.059</b>	AVG.	CIFAR-10	DenseNet	.38

### 3.1.1 Memorisation of unique features in MLPs

Now we proceed with the more practical black box setting where we do not know the training data or the canaries’ label. We measure  $M$  for the 15 highest and the 15 lowest self-influence training examples. See Section A for additional training details. Table 2 shows the top-3  $M$  canaries, and the average  $M$  score over canaries with  $M > 0$  per dataset. We will use the average memorisation score as a comparison between model architectures where the choice of canaries varies. The variation occurs because canaries are chosen by the self-influence score which depends on the model architecture. We report on the effect of self-influence on  $M$  in Section 3.3.

### 3.1.2 Memorisation of unique features in CNNs

Here we investigate memorisation in CNNs in a black-box setting. Table 2 shows the top-3  $M$  canaries and the averaged  $M$  score for canaries with  $M > 0$ . Average memorisation appears greater in a CNN as opposed to an MLP architecture for MNIST ( $0.012 > 0.0013$ ) and Fashion-MNIST ( $0.028 > 0.0093$ ). In fact, average memorisation in CNNs is over an order of magnitude greater than MNIST. It also seems that the average memorisation is greater for CIFAR-10 in DenseNet than in CNN-2 ( $0.38 > 0.018$ ), however, the sample size for the DenseNet results is small. Similarly to Feldman and Zhang (2020), networks with higher validation accuracies appear to show greater memorisation (DenseNet and CNN-2 have a validation accuracies of  $\approx 92\%$  and  $\approx 72\%$  respectively).

## 3.2 Effects of explicit and implicit regularisation on memorisation

We now explore how explicit and implicit regularisation strategies affect unique feature memorisation. We consider three regularisation strategies: dropout, data augmentation, and batch normalisation, applied in various combinations. See Section A for details on the regularisers.

Table 3 shows the average memorisation score for canaries where  $M > 0$ . The results, taking MNIST for example, illustrate that almost all values are higher than the average of 0.0013 obtained from Table 2 without any regularisation. We find that there is no statistically significant difference in the average memorisation scores when the regularisers are used to train MLP-1 on F-MNIST. Canaries in CIFAR-10 have greater memorisation scores than in the non-regularised models shown in Table 2. These results extend to the level of features, findings that have been made previously for the memorisation of whole training examples (Zhang et al., 2021a).

Data augmentation increases memorisation. The average memorisation increases from 0.018 to 0.13 for CNN-2 trained on CIFAR-10 with data augmentation. We suggest this is because at every epoch a different perturbed canary is used to train the model. This increase in the number of effective canaries increases the spurious correlation between the unique feature and label and thus enables easier learning of the feature.

Table 3: Average memorisation ( $M$ ) scores over canaries with  $M > 0$  for unique features for models with explicit and implicit regularisers, such as Dropout, Data Augmentation, and Batch Normalisation.

$D_t$	MODEL	REGULARISATION	$M$
MNIST	MLP-1	Dropout	.02
MNIST	MLP-1	Data Augmentation	.0033
MNIST	MLP-1	Dropout & Data Augmentation	.0013
MNIST	MLP-1	Batch Normalisation	.039
F-MNIST	MLP-1	Dropout	.025
F-MNIST	MLP-1	Data Augmentation	.0065
F-MNIST	MLP-1	Dropout & Data Augmentation	.029
F-MNIST	MLP-1	Batch Normalisation	.00097
CIFAR-10	CNN-2	Dropout	.38
CIFAR-10	CNN-2	Data Augmentation	.13
CIFAR-10	CNN-2	Dropout & Data Augmentation	.44
CIFAR-10	CNN-2	Batch Normalisation	1.7

### 3.3 Characterisation of unique feature memorisation

Our results show that neural networks memorise unique features that occur once in a training dataset, and that regularisation strategies do not help to reduce this behaviour. These results are intriguing and lead us to consider the following questions to characterise unique feature memorisation.

*Is memorisation influenced by sample complexity?* We find a weak correlation between self-influence and  $M$  for the top-15, bottom-15  $M$  score canaries in MNIST for MLP-1 (Pearson’s correlation coefficient 0.43). And we find no correlation for F-MNIST and CIFAR-10. These results indicate that sample complexity (alone) does not provide an adequate explanation for unique feature memorisation. Next, we explore other possible factors affecting memorisation, such as the stochasticity of the learning algorithm or changes in sample self-influence after a feature has been added.

*Is memorisation affected by training stochasticity?* Yes, we find that unique feature memorisation is affected by the training seed. We use the white box setting to isolate this result from the  $M$  score. Figure 3(a) shows the range of memorisation scores for 30 randomly selected MNIST canaries over training runs with different random seeds. (Results for 100 canaries in MNIST and CIFAR-10 are given in Section B.2. Positive and negative  $M_w$  scores show the randomness in memorisation.

*Does having a unique feature make for a high self-influence sample?* We examine the self-influence of samples with and without the unique feature. First, we measure the self-influence of all samples in MNIST using TracIn. Then, we select the highest and lowest influence sample and inject the unique feature. Then, we re-train the model and measure the self-influence of these canaries using the same seed. We find that the influence of the low influence sample increases hugely from  $1.0 \times 10^{-13}$  to  $7.5 \times 10^4$ . A high influence sample sees modest increase in influence from  $6.6 \times 10^4$  to  $7.5 \times 10^4$ . These results show that the addition of the unique feature creates a highly influential sample even when the sample’s other features were easy to learn from other samples.

*Where does memorisation happen in neural networks?* Baldock et al. (2021) showed that sample memorisation occurs deep in neural networks. Here in a white box setting (i.e. access to model activations) we show that MLPs extract a latent representation for the unique feature in the layer before the softmax. We describe how we find this latent in Section B. Figure 3(b) shows activations for inferences on  $\mathbf{z}_u$  (unique) and  $\mathbf{z}_r$  (random). Crucially, only the unique feature activates the latent at index 41. This latent is extracted only for the unique feature and not the random feature  $\mathbf{z}_r$ . Instead, the latent at index 175 is activated by both patches suggesting that this feature represents activations in the location of the patch in the image space.

*Do unique features get memorised early on?* Figure 3(c) offers a profile of  $M$  during training. In agreement with Carlini et al. (2019b); Van den Burg and Williams (2021) our results show that unique feature memorisation begins early, and therefore that early stopping does not prevent memorisation.

*Why are unique features memorised?* Collectively our results show that unique feature memorisation is not a property of the underlying sample complexity, and that learning on this sample is greatly

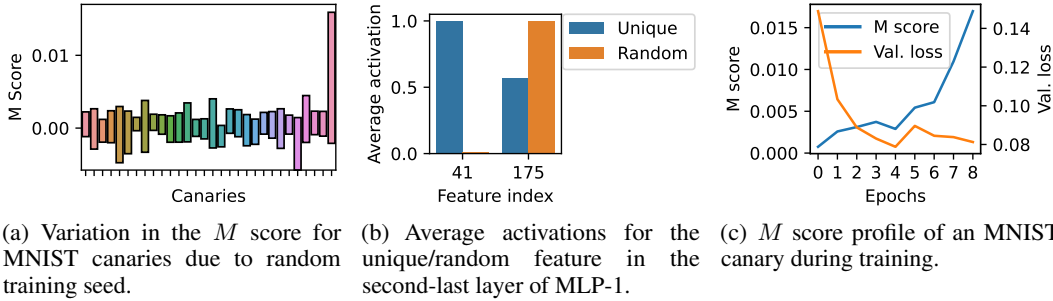


Figure 3: Characterisations of unique feature memorisation in MLP-1 trained on MNIST.

influenced by the addition of a unique feature. Typically, we would expect the learning algorithm to ignore the unique feature. This is because under the information bottleneck (IB) principle, information learnt from the other samples in the training dataset is sufficient to reduce the uncertainty on the label distribution (Tishby and Zaslavsky, 2015; Achille and Soatto, 2018).

However, in practice this does not seem to be the case. We suggest the following explanation for this behaviour. Let us assume that the classifier is extracting a latent space from the input data. We can theoretically partition the latents in two parts: those learned from the samples according to the IB principle and those attributed to the unique feature. Indeed our results in Figure 3(b) hint at this. On the latents extracted from the unique feature the classification task is easy: the canary is linearly separable from all samples as these latents are not shared by any other sample. Under the *Principle of Least Effort* (Geirhos et al., 2020), the learning algorithm may shortcut over the unique feature since it is easy to learn, and as our results suggest it may do so early on in training (Figure 3(c)). The stochasticity observed in our findings (Figure 3(a)), suggests that the decision as to whether the shortcut is learnt is a random process and may relate to the initialisation weights or when the canary is presented to the learning algorithm in stochastic mini-batch gradient descent or other gradient dynamics effects (Pezeshki et al., 2020).

## 4 Related Work

To the best of our knowledge, no previous study has investigated methods that detect memorisation of single unique features in image classification models in the stringent settings we consider. However, existing research recognises the critical role that memorisation plays in the overfitting and generalisation of neural networks and the security implications of attacks using adversarial training examples. Below we outline work that has provided encouraging findings to help us shape this work.

### 4.1 Memorisation

The main objective of this work is to understand whether memorisation occurs for unique features that occur *once* per dataset and are located on a single training example.

Previous work has established that over-trained, over-parameterised neural networks memorise training labels (Zhang et al., 2021a). Several metrics for assessing the memorisation of training labels have been introduced (Feldman and Zhang, 2020; Jiang et al., 2021). It was shown that DNNs first learn common patterns in training examples, after which they memorise labels (Arplt et al., 2017; Kim et al., 2018b). More recently, it has been shown that learning and memorisation occur simultaneously (Liu et al., 2021b). These works show that regularisation does not eliminate memorisation. We take inspiration from Zhang et al. (2021a) and explore whether the regularisation prevents unique feature memorisation.

Privacy attacks are methods that exploit data leakage to uncover information about training data. For example, membership inference attacks deduce whether a sample is in the training set by exploiting a model’s overconfidence on examples it has seen (Shokri et al., 2017; Sablayrolles et al., 2018; Salem et al., 2018; Liu and Tsafaris, 2020; Choquette-Choo et al., 2021). We propose that models leak



information about unique features. And we focus on the memorisation of unique features and not whole data.

Recent work by Carlini et al. (2019b, 2021) established that LLMs memorise features. Unique sequences, such as credit card numbers or rarely occurring phrases are random and therefore cannot be *learnt* from similar patterns in the remainder of the training data. The authors developed *exposure* as a black box inference method to measure feature memorisation. This work has inspired us to draw upon the use of canaries to measure the memorisation of unique features in images. We follow their idea to also explore memorisation before *over-learning* occurs. However, our work is different to measuring feature memorisation in LLMs. In discriminative models we cannot measure the propensity of a unique feature, and other theoretically equally likely features from the softmax outputs, and thus we cannot calculate the exposure of the canary. Also in LLMs the feature’s label is self-evident, whereas the under the same assumption we do not know the unique feature’s label in the discriminate setting. This makes memorisation harder to measure.

Property inference attacks attempt to learn a group property/feature of the dataset. For example, what proportion of people in the training set wear glasses? (Ateniese et al., 2015; Ganju et al., 2018). These attacks are typically white box and proceed by using a shadow model to make inferences on the target model weights. Feature memorisation, as we investigate here, can be viewed as an extreme property inference attack where a unique feature, a person who wears glasses, occurs only once in the dataset. Existing approaches, however, cannot address unique feature memorisation since labelling the training weights to train the shadow model requires ground-truth knowledge of whether the feature was memorised or not.

We also draw upon the idea of concept activation vectors (CAV), as introduced by Kim et al. (2018a), to infer the sensitivity of the network to the feature we are interested in vs. random features that we are not. However, instead of image concepts such as stripes, we focus on unique features and use only the outputs of the trained model as opposed to the internal activations of the network. Our memorisation score also does not require the label of the unique feature.

A concurrent work by Yang and Chaudhuri (2022) show in a white box setting that neural network image classifiers learn rare features when they occur *three or more* times in the training data. We instead develop a method which does not require access to training data and show that memorisation occurs even for a *single* unique feature in the training data.

## 4.2 Backdoor attacks

Backdoor attacks are fundamentally different to our work. These attacks attempt to adversarially change a model’s predictions by injecting an optimised image patch onto training examples such that when this patch occurs on an attack example at test time, the predictions of the model can be controlled (Chen et al., 2017; Gu et al., 2017; Liu et al., 2018; Muñoz-González et al., 2017; Shafahi et al., 2018; Saha et al., 2019). In contrast, we show that a unique feature which occurs in the training data is memorised. This feature is not optimised to modify the outputs of the model at test time.

## 5 Conclusion

We present a score to measure the memorisation of unique features in imaging datasets by neural network image classification models. We focus on the case where the unique feature appears on a single image in the training data, and where we have access to the the unique feature, but not to the training data or the model weights.

We show that unique feature memorisation occurs in this setting, and is not eliminated by typical explicit and implicit regularisation strategies, dropout, data augmentation and batch normalisation. We derive these results for benchmark datasets and a range of neural network architectures. We also show that unique feature memorisation occurs early in training, and that MLPs extract representations for these features.

**Social impact** These results, even in standard benchmark datasets, suggest that neural networks pose a privacy risk to unique sensitive information in imaging datasets even if the information occurs once. The information does not have to be rare in the wild. In the context of a healthcare application, the information could be a patient name that was not removed by an image pre-processor.

## 6 Acknowledgements

This work is supported by iCAIRD, which is funded by Innovate UK on behalf of UK Research and Innovation (UKRI) [project number 104690]. S.A. Tsafaris acknowledges also support by a Canon Medical / Royal Academy of Engineering Research Chair under Grant RCSR1819\8\25. This work was partially supported by the Alan Turing Institute under EPSRC grant EP/N510129/1.

## References

- Achille, A. and Soatto, S. (2018). Emergence of invariance and disentanglement in deep representations. *J. Mach. Learn. Res.*, 19(1):1947–1980.
- Arplt, D., Jastrzebski, S., Bailas, N., Krueger, D., Bengio, E., Kanwal, M. S., Maharaj, T., Fischer, A., Courville, A., Bengio, Y., and Lacoste-Julien, S. (2017). A closer look at memorization in deep networks. *34th International Conference on Machine Learning, ICML 2017*, 1:350–359.
- Ateniese, G., Mancini, L. V., Spognardi, A., Villani, A., Vitali, D., and Felici, G. (2015). Hacking smart machines with smarter ones: How to extract meaningful data from machine learning classifiers. *Int. J. Secur. Netw.*, 10(3):137–150.
- Atienza, R. (2022). Advanced-Deep-Learning-with-Keras.
- Baldock, R. J. N., Maennel, H., and Neyshabur, B. (2021). Deep Learning Through the Lens of Example Difficulty.
- Bar, Y., Diamant, I., Wolf, L., Lieberman, S., Konen, E., and Greenspan, H. (2015). Chest pathology detection using deep learning with non-medical training. In *2015 IEEE 12th International Symposium on Biomedical Imaging (ISBI)*, pages 294–297.
- Carlini, N., Erlingsson, U., and Papernot, N. (2019a). Prototypical Examples in Deep Learning: Metrics, Characteristics, and Utility.
- Carlini, N., Liu, C., Erlingsson, U., Kos, J., and Song, D. (2019b). The secret sharer: Evaluating and testing unintended memorization in neural networks. In *Proceedings of the 28th USENIX Conference on Security Symposium, SEC’19*, page 267–284, USA.
- Carlini, N., Tramer, F., Wallace, E., Jagielski, M., Herbert-Voss, A., Lee, K., Roberts, A., Brown, T., Song, D., Erlingsson, U., et al. (2021). Extracting training data from large language models. In *30th USENIX Security Symposium (USENIX Security 21)*, pages 2633–2650.
- Chen, X., Liu, C., Li, B., Lu, K., and Song, D. (2017). Targeted backdoor attacks on deep learning systems using data poisoning.
- Choquette-Choo, C. A., Tramer, F., Carlini, N., and Papernot, N. (2021). Label-only membership inference attacks. In *International Conference on Machine Learning*, pages 1964–1974. PMLR.
- DeGrave, A. J., Janizek, J. D., and Lee, S. I. (2021). AI for radiographic COVID-19 detection selects shortcuts over signal. *Nature Machine Intelligence*, 3(7):610–619.
- Feldman, V. (2020). Does learning require memorization? a short tale about a long tail. In *Proceedings of the 52nd Annual ACM SIGACT Symposium on Theory of Computing*, pages 954–959.
- Feldman, V. and Zhang, C. (2020). What Neural Networks Memorize and Why: Discovering the Long Tail via Influence Estimation. In Larochelle, H., Ranzato, M., Hadsell, R., Balcan, M. F., and Lin, H., editors, *Advances in Neural Information Processing Systems*, volume 33, pages 2881–2891.
- Ganju, K., Wang, Q., Yang, W., Gunter, C. A., and Borisov, N. (2018). Property Inference Attacks on Fully Connected Neural Networks Using Permutation Invariant Representations. In *Proceedings of the 2018 ACM SIGSAC Conference on Computer and Communications Security, CCS ’18*, pages 619–633.
- Garima, Liu, F., Kale, S., and Sundararajan, M. (2020). Estimating training data influence by tracing gradient descent. *Advances in Neural Information Processing Systems*, 2020-Decem.

- Garima, Liu, F., Kale, S., and Sundararajan, M. (2022). TrackIn FAQ.
- Geirhos, R., Jacobsen, J. H., Michaelis, C., Zemel, R., Brendel, W., Bethge, M., and Wichmann, F. A. (2020). Shortcut learning in deep neural networks. *Nature Machine Intelligence*, 2(11):665–673.
- Ghorbani, A. and Zou, J. (2019). Data shapley: Equitable valuation of data for machine learning. *36th International Conference on Machine Learning, ICML 2019*, 2019-June:4053–4065.
- Golatkar, A., Achille, A., and Soatto, S. (2020). Eternal sunshine of the spotless net: Selective forgetting in deep networks. *Proceedings of the IEEE Computer Society Conference on Computer Vision and Pattern Recognition*, pages 9301–9309.
- Gu, T., Dolan-Gavitt, B., and Garg, S. (2017). Badnets: Identifying vulnerabilities in the machine learning model supply chain.
- Guo, H., Rajani, N. F., Hase, P., Bansal, M., and Xiong, C. (2020). FastIF: Scalable Influence Functions for Efficient Model Interpretation and Debugging.
- Harutyunyan, H., Achille, A., Paolini, G., Majumder, O., Ravichandran, A., Bhotika, R., and Soatto, S. (2021). Estimating informativeness of samples with smooth unique information. In *International Conference on Learning Representations*.
- Huang, G., Liu, Z., van der Maaten, L., and Weinberger, K. Q. (2018). Densely connected convolutional networks.
- Idrissi, B. Y., Arjovsky, M., Pezeshki, M., and Lopez-Paz, D. (2021). Simple data balancing achieves competitive worst-group-accuracy. 140:1–14.
- Jedorova, M., Kaul, C., Mayor, C., O’Neil, A. Q., Weir, A., Murray-Smith, R., and Tsaftaris, S. A. (2021). Survey: Leakage and privacy at inference time.
- Jiang, Z., Zhang, C., Talwar, K., and Mozer, M. C. (2021). Characterizing structural regularities of labeled data in overparameterized models. In Meila, M. and Zhang, T., editors, *Proceedings of the 38th International Conference on Machine Learning*, volume 139 of *Proceedings of Machine Learning Research*, pages 5034–5044. PMLR.
- Katharopoulos, A. and Fleuret, F. (2018). Not All Samples Are Created Equal: Deep Learning with Importance Sampling. In Dy, J. and Krause, A., editors, *Proceedings of the 35th International Conference on Machine Learning*, volume 80 of *Proceedings of Machine Learning Research*, pages 2525–2534. PMLR.
- Kim, B., Wattenberg, M., Gilmer, J., Cai, C., Wexler, J., Viegas, F., et al. (2018a). Interpretability beyond feature attribution: Quantitative testing with concept activation vectors (tcav). In *International conference on machine learning*, pages 2668–2677. PMLR.
- Kim, Y., Kim, M., and Kim, G. (2018b). Memorization precedes generation: Learning unsupervised GANs with memory networks. In *International Conference on Learning Representations*.
- Kingma, D. P. and Ba, J. (2015). Adam: A method for stochastic optimization. In *ICLR (Poster)*.
- Koh, P. W. and Liang, P. (2017). Understanding black-box predictions via influence functions. In *Proceedings of the 34th International Conference on Machine Learning - Volume 70, ICML’17*, page 1885–1894.
- Krizhevsky, A., Hinton, G., et al. (2009). Learning multiple layers of features from tiny images.
- Krueger, D., Ballas, N., Jastrzebski, S., Arpit, D., Kanwal, M. S., Maharaj, T., Bengio, E., Fischer, A., and Courville, A. (2019). Deep nets don’t learn via memorization. *5th International Conference on Learning Representations, ICLR 2017 - Workshop Track Proceedings*, pages 1–4.
- Lecun, Y., Bottou, L., Bengio, Y., and Haffner, P. (1998). Gradient-based learning applied to document recognition. *Proceedings of the IEEE*, 86(11):2278–2324.

- Liu, E. Z., Haghighi, B., Chen, A. S., Raghunathan, A., Koh, P. W., Sagawa, S., Liang, P., and Finn, C. (2021a). Just train twice: Improving group robustness without training group information. In *Proceedings of the 38th International Conference on Machine Learning*, volume 139, pages 6781–6792. PMLR.
- Liu, F., Lin, T., and Jaggi, M. (2021b). Understanding Memorization from the Perspective of Optimization via Efficient Influence Estimation. pages 1–14.
- Liu, J., Sun, Y., Han, C., Dou, Z., and Li, W. (2020). Deep representation learning on long-tailed data: A learnable embedding augmentation perspective. In *Proceedings of the IEEE/CVF Conference on Computer Vision and Pattern Recognition (CVPR)*.
- Liu, X. and Tsiftaris, S. A. (2020). Have you forgotten? A method to assess if machine learning models have forgotten data. In *International Conference on Medical Image Computing and Computer-Assisted Intervention*, pages 95–105. Springer.
- Liu, Y., Ma, S., Aafer, Y., Lee, W.-C., Zhai, J., Wang, W., and Zhang, X. (2018). Trojaning attack on neural networks. In *NDSS*.
- Muñoz-González, L., Biggio, B., Demontis, A., Paudice, A., Wongrassamee, V., Lupu, E. C., and Roli, F. (2017). Towards Poisoning of Deep Learning Algorithms with Back-gradient Optimization. In *Proceedings of the 10th ACM Workshop on Artificial Intelligence and Security*, pages 27–38.
- Pezeshki, M., Kaba, S.-O., Bengio, Y., Courville, A., Precup, D., and Lajoie, G. (2020). Gradient starvation: A learning proclivity in neural networks. *arXiv preprint arXiv:2011.09468*.
- Sablayrolles, A., Douze, M., Schmid, C., and Jégou, H. (2018). Deja Vu: an empirical evaluation of the memorization properties of ConvNets. (2015):1–22.
- Saha, A., Subramanya, A., and Pirsiavash, H. (2019). Hidden trigger backdoor attacks.
- Salem, A., Zhang, Y., Humbert, M., Berrang, P., Fritz, M., and Backes, M. (2018). ML-Leaks: Model and Data Independent Membership Inference Attacks and Defenses on Machine Learning Models.
- Shafahi, A., Huang, W. R., Najibi, M., Suci, O., Studer, C., Dumitras, T., and Goldstein, T. (2018). Poison frogs! targeted clean-label poisoning attacks on neural networks.
- Shao, L., Song, Y., and Ermon, S. (2020). Understanding classifier mistakes with generative models.
- Shokri, R., Stronati, M., Song, C., and Shmatikov, V. (2017). Membership inference attacks against machine learning models. In *2017 IEEE Symposium on Security and Privacy (SP)*, pages 3–18. IEEE.
- Tishby, N. and Zaslavsky, N. (2015). Deep learning and the information bottleneck principle. In *2015 IEEE Information Theory Workshop (ITW)*, pages 1–5.
- Toneva, M., Trischler, A., Sordani, A., Bengio, Y., Des Combes, R. T., and Gordon, G. J. (2019). An empirical study of example forgetting during deep neural network learning. *7th International Conference on Learning Representations, ICLR 2019*, pages 1–19.
- Van den Burg, G. J. J. and Williams, C. K. I. (2021). On memorization in probabilistic deep generative models. In *Advances in Neural Information Processing Systems*, volume 34.
- Wikipedia (2022). Chest radiograph — Wikipedia, the free encyclopedia. [https://en.wikipedia.org/wiki/Chest\\_radiograph#/media/File:Normal\\_posteroanterior\\_\(PA\)\\_chest\\_radiograph\\_\(X-ray\).jpg](https://en.wikipedia.org/wiki/Chest_radiograph#/media/File:Normal_posteroanterior_(PA)_chest_radiograph_(X-ray).jpg). [Online; accessed 17-January-2022].
- Xiao, H., Rasul, K., and Vollgraf, R. (2017). Fashion-mnist: a novel image dataset for benchmarking machine learning algorithms.
- Yang, Y.-Y. and Chaudhuri, K. (2022). Understanding rare spurious correlations in neural networks.
- Zech, J. R., Badgeley, M. A., Liu, M., Costa, A. B., Titano, J. J., and Oermann, E. K. (2018). Variable generalization performance of a deep learning model to detect pneumonia in chest radiographs: A cross-sectional study. *PLoS Medicine*, 15(11):1–17.

Zhang, C., Bengio, S., Hardt, M., Recht, B., and Vinyals, O. (2021a). Understanding deep learning (still) requires rethinking generalization. *Commun. ACM*, 64(3):107–115.

Zhang, Y., Kang, B., Hooi, B., Yan, S., and Feng, J. (2021b). Deep long-tailed learning: A survey.

## A Models and training

### A.1 Datasets

We choose three benchmarked datasets to train the image classification models. MNIST is a 10 class set of handwritten digits with image size  $28 \times 28 \times 1$  (Lecun et al., 1998), F-MNIST is a 10 class set clothing thumbnails with image size  $28 \times 28 \times 1$  (Xiao et al., 2017) and CIFAR-10 is a 10 class set of common objects with image size  $32 \times 32 \times 3$  (Krizhevsky et al., 2009). We use the original train/test splits given by the dataset authors.

We use CIFAR-10 as an OOD dataset to evaluate the M-score for models trained on MNIST and F-MNIST, and to evaluate models trained on CIFAR-10, we use a resized, 3-channel version of MNIST. To perform image transformations we use the `tf.image` API in TensorFlow v2.7.

### A.2 Training strategy

All models are trained to reduce overlearning. To do this we make use of using early stopping. We train up to 500 epochs with a patience of 10 epochs. After training, we select the final model weights from the epoch with the lowest validation loss. We use the Adam optimiser and a cross-entropy loss function (Kingma and Ba, 2015).

To train and evaluate models we use TensorFlow 2.7. We train models using an Nvidia<sup>®</sup> Titan RTX<sup>™</sup>. A low-carbon and renewable energy source was provided by The University of Edinburgh. We estimate the computation time for the experiments to be around 200 GPU hours.

### A.3 Network architectures

We evaluate our memorisation score using several common architectural styles of neural networks. The first, *MLP-1* is trained on MNIST and Fashion-MNIST datasets. It is comprised of: Dense(512)  $\rightarrow$  ReLU  $\rightarrow$  Dense(256)  $\rightarrow$  ReLU  $\rightarrow$  Dense(128)  $\rightarrow$  ReLU  $\rightarrow$  Dense(#classes)  $\rightarrow$  Softmax.

We train MLP-1 with a learning rate of  $3 \times 10^{-4}$  and a batch size of 128.

CNN-1 a simple 2-layer convolutional neural network. It is comprised of: Conv2D(32,3,3)  $\rightarrow$  ReLU  $\rightarrow$  Conv2D(64,3,3)  $\rightarrow$  MaxPool2d(2,2)  $\rightarrow$  ReLU  $\rightarrow$  Dense(128)  $\rightarrow$  ReLU  $\rightarrow$  Dense(128)  $\rightarrow$  ReLU  $\rightarrow$  Dense(#classes)  $\rightarrow$  Softmax.

We train CNN-1 with a learning rate of  $3 \times 10^{-4}$  and a batch size of 128.

CNN-2 is small VGG-style network trained on CIFAR-10. It is comprised of: Conv2D(32,3,3)  $\rightarrow$  ReLU  $\rightarrow$  Conv2D(32,3,3)  $\rightarrow$  ReLU  $\rightarrow$  MaxPool2d(2,2)  $\rightarrow$  Conv2D(64,3,3)  $\rightarrow$  ReLU  $\rightarrow$  Conv2D(64,3,3)  $\rightarrow$  ReLU  $\rightarrow$  MaxPool2d(2,2)  $\rightarrow$  Dense(1024)  $\rightarrow$  ReLU  $\rightarrow$  Dense(#classes)  $\rightarrow$  Softmax.

We train CNN-2 with a learning rate of  $3 \times 10^{-4}$  and a batch size of 512.

*DenseNet* is DenseNet trained on CIFAR-10 Huang et al. (2018). The network has 100 layers, a growth factor of 12, and three dense blocks. We use an existing implementation and train using the same parameters given in Atienza (2022).

### A.4 Regularisation strategies

We sample new data augmentations for every mini-batch that we train. For MNIST and F-MNIST three augmentations. We randomly adjust the contrast by a factor of 0.2 and we apply random cropping (27, 27) so that we ensure we do not remove the unique features from the image. For CIFAR-10 we also include random horizontal flipping.

We use dropout in MLPs and CNNs. For each mini-batch we reduce the connections in fully connected layers by a factor of 0.2, and in CNN layers we reduce by a factor of 0.5. No dropout is applied to the softmax layer. Batch normalisation is applied directly before the activation layer in all layers in MLP-1 and the CNNs except for the softmax layer. We use momentum = 0.99 and  $\epsilon = 0.001$ .

### A.5 Computing self-influence using TracIn

We determine the self-influence of samples using TracIn. TracIn measures the self-influence of an example by computing the difference in training loss with respect to itself between successive iterations of stochastic gradient descent (SGD) where the loss is computed on that example. We use an approximation, TracInCP, which approximates TracIn for SGD with mini-batches. It is computed at user specified checkpoints given by

$$\text{TracInCP} = \sum_i^n \eta_i \|\nabla l(\mathbf{w}_i, \mathbf{x})\|^2, \tag{2}$$

where  $\mathbf{w}_i$  and  $\eta_i$  are the weights and learning rate of  $f$  and the optimisation algorithm at checkpoint  $i$  to  $n$ ,  $\mathbf{x}$  image whose self influence we want to measure.

For each black box experiment in this work, we measure the self-influence of all training examples by selecting 10 evenly spaced checkpoints which account for a 95% reduction in the training loss (Garima et al., 2022). We select the top-15 and bottom-15 examples as canaries. We create 30 models, each of which is trained on the canary that has been injected with a unique feature.

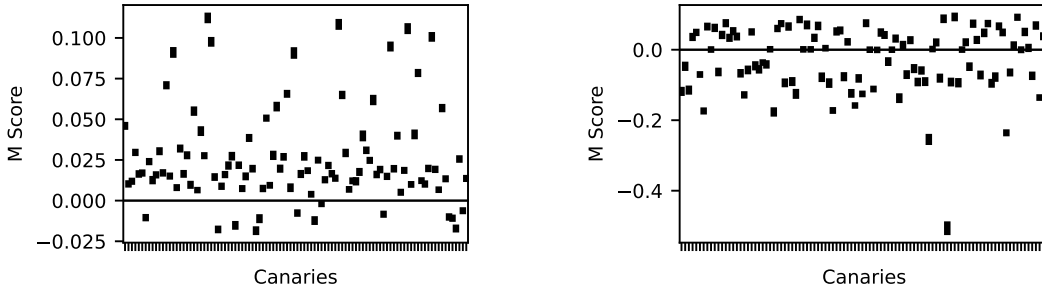
### A.6 Finding a latent represent of the unique feature in an MLP

We train 100 MLP models with a fixed seed using a randomly selected canary per model. We perform inferences using the training data containing the unique feature and the clean OOD image pairs, and record the activations in the second-last layer. Next, we threshold the activations such any non-zero activation is equal to one. Since ReLU activations are used, the remaining activations are zero. We subtract the clean activations from the unique feature activations and repeat the thresholding operation. In this way we measure activations only excited by the unique feature patch. Next, we average over the activations map for each model and normalise. We obtain the most commonly excited activations marginalised over the choice of canary.

## B Additional experiments

### B.1 Memorisation in a white box setting

In this experiment we show the memorisation scores for 100 randomly selected MNIST and CIFAR-10 canaries for MLP-1 and CNN-2 respectively. We measure the memorisation scores for three evaluations of  $M_w$ . In each evaluation we sample a different set of random features to inject into the OOD examples, and we use all the samples in the OOD dataset. Each evaluation acts on the same trained model. In Figure 4 for we show the results for the mean  $M_w$  score and one standard deviation.



(a) M Score for 100 randomly chosen MNIST samples used to train MLP-1.

(b) M Score for 100 randomly chosen CIFAR-10 samples used to train CNN-2.

Figure 4: M scores for the unique feature patch on 100 randomly chosen canaries. Each datapoint represents the M score for a single canary in a training dataset used to train a single model. We show the standard deviation of the M score of three evaluations.

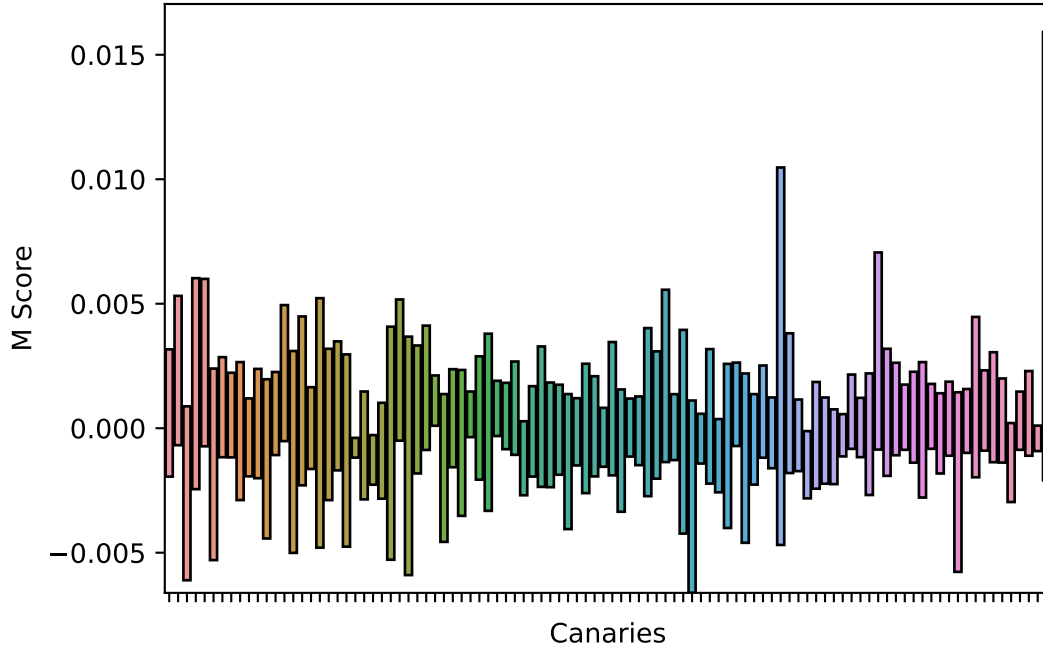


Figure 5: Range in the  $M$  score for MNIST canaries across five training runs.

## B.2 Effect of learning algorithm on memorisation

In this experiment we measure  $M$  for 100 randomly selected canaries over five training runs. We train 100 models, one for each canary, and we repeat the training five times using different random seeds. The  $M$  score uses the same random seed for each evaluation. We train MLP-1 on MNIST and CNN-2 on CIFAR-10. We calculate the range of  $M$  over the training runs. The results are shown in Figure 5 and 6 respectively. Both figures show that  $M$  has positive and negative results in different training runs for the same canaries. This shows that memorisation varies depending on the randomness of the learning algorithm. Also the range of the  $M$  score over training runs is far greater than the range due to the stochasticity of the memorisation score in Section B.1. This shows that the variation due to the learning algorithm is greater than the precision of the memorisation score.



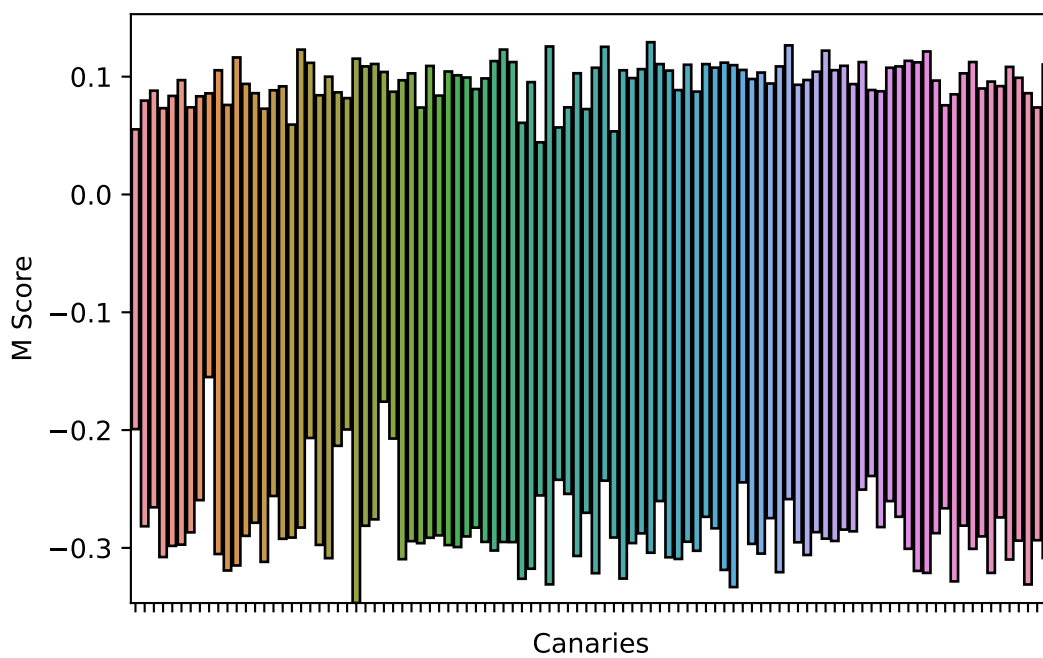


Figure 6: Range in the  $M$  score for CIFAR-10 canaries across five training runs.